

The Unusual Redox Properties of Fluoroferrrocenes Revealed through a Comprehensive Study of the Haloferrrocenes

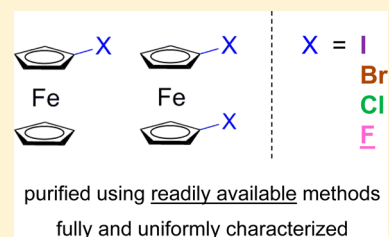
Michael S. Inkpen,^{†,§} Shuoren Du,^{†,‡,§} Mariana Hildebrand,[†] Andrew J. P. White,[†] Nicholas M. Harrison,[†] Tim Albrecht,^{*,†} and Nicholas J. Long^{*,†}

[†]Department of Chemistry, Imperial College London, London, SW7 2AZ, U.K.

[‡]College of Chemistry and Molecular Engineering, Peking University, Beijing, 100871, China

S Supporting Information

ABSTRACT: We report the synthesis and full characterization of the entire haloferrrocene (FcX) and 1,1'-dihaloferrrocene (fcX₂) series (X = I, Br, Cl, F; Fc = ferrocenyl, fc = ferrocene-1,1'-diyl). Finalization of this simple, yet intriguing set of compounds has been delayed by synthetic challenges associated with the incorporation of fluorine substituents. Successful preparation of fluoroferrrocene (FcF) and 1,1'-difluoroferrrocene (fcF₂) were ultimately achieved using reactions between the appropriate lithiated ferrocene species and *N*-fluorobenzenesulfonimide (NFSI). The crude reaction products, in addition to those resulting from analogous preparations of chloroferrrocene (FcCl) and 1,1'-dichloroferrrocene (fcCl₂), were utilized as model systems to probe the limits of a previously reported “oxidative purification” methodology. From this investigation and careful solution voltammetry studies, we find that the fluorinated derivatives exhibit the *lowest* redox potentials of each of the FcX and fcX₂ series. This counterintuitive result is discussed with reference to the spectroscopic, structural, and first-principles calculations of these and related materials.



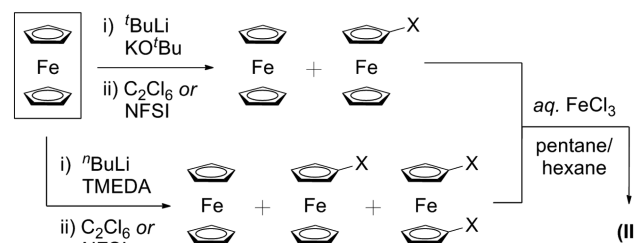
INTRODUCTION

The first synthetic routes to haloferrrocenes (FcX) and 1,1'-dihaloferrrocenes (fcX₂) were reported only 4 years after the discovery of ferrocene itself (X = I, Br, Cl, F; fc = ferrocene-1,1'-diyl, Fc = ferrocenyl).¹ In the subsequent 60 years, these precursors have been reacted to form a wide variety of useful materials including redox-active ligands,² polymers,³ or model systems for the study of charge transfer.⁴ In the published literature, a remarkable omission from this series is 1,1'-difluoroferrrocene (fcF₂), although we note several preparative attempts have been described.⁵ Furthermore, until very recently⁶ the only known methods to synthesize fluoroferrrocene (FcF) utilized *explosive* perchloryl fluoride^{14,7} or *toxic* mercurated materials.⁸ Perhaps as a result, to the best of our knowledge, only three other ferrocenes comprising a Cp–F bond are known: 2-fluoro[(dimethylamino)methyl]ferrocene,^{7a} 1-fluoro-2-(2-pyridyl)ferrocene,⁹ and 1,2,3,4,5-pentafluoroferrrocene.⁶ To date, there are more known examples of fluorinated ruthenocenes (~11 complexes¹⁰) and no reports of fluorinated osmocenes. Despite significant interest, it has not yet proved possible to synthesize any perfluorometalloenes.¹¹ In this work, we corroborate a safer approach for the preparation of FcF and communicate a synthetic route to fcF₂ (Scheme 1).

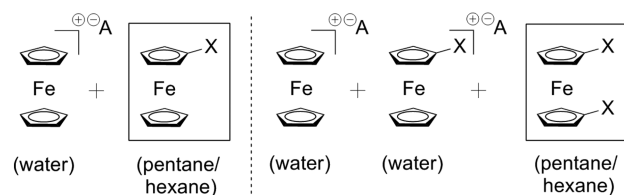
Historically, investigations into chlorinated and fluorinated metalloenes have been motivated by their potential applications as polymeric/structural materials with combined thermal, radiation, and oxidation resistance.^{11a,13} Our initial interest lay in the use of these materials as models to explore the limits of a previously reported “oxidative purification”

Scheme 1. Synthesis and Oxidative Purification of FcCl and FcF (Top/Left) and fcCl₂ and fcF₂ (Bottom/Right)^a

(I) Synthesis



(II) Oxidative purification



^aNFSI = *N*-fluorobenzenesulfonimide; X = Cl, F; A[−] = Cl[−], [FeCl₃][−](aq), or [FeCl₄][−](aq).¹²

technique.¹⁴ The latter can be used to separate redox-active mixtures of similar polarity that are typically difficult to purify using conventional techniques (for example, chromatography

Received: September 24, 2015

or recrystallization). By washing *n*-alkane solutions comprising FcH and FcX (or FcH, FcX, and fcX₂) with aqueous solutions of FeCl₃ made up to appropriate concentrations, components of each mixture can be oxidized sequentially. We,^{14c} and others,^{14b} have observed that the resulting [FcH]⁺A⁻ (or [FcH]⁺A⁻ and [FcX]⁺A⁻) species are water-soluble and easily extracted (X = I, Br; A⁻ = Cl⁻, [FeCl₃]⁻(aq), or [FeCl₄]⁻(aq)),¹² leaving only the complex with the highest redox potential dissolved in the organic phase. This methodology is conceptually similar to pioneering work of Cunningham and McMillin.^{14a} Given the success of this approach, it was of interest to determine the maximum equilibrium potential that can be utilized with the biphasic aqueous FeCl₃/*n*-alkane system. This is however not trivial, as reactions are likely occurring at the solution–solution interface. We considered that an approximate limit might be deduced by extending the purification approach to the entire FcX and fcX₂ series (providing a range of equilibrium potentials for testing). Given the high electronegativity of fluorine, it was hypothesized that fcF₂ would be the most difficult to oxidize of all. Remarkably, we instead found FcF and fcF₂ to be the easiest to oxidize of the FcX and fcX₂ series. This unexpected result and its implications are discussed with reference to the experimental, structural, and first-principles calculations of these and related materials. (We note that during the preparation of this article, a related study was published that corroborates our findings.¹⁵)

RESULTS AND DISCUSSION

a. Synthesis and “Oxidative Purification”. The synthesis of most monohalo- and 1,1'-dihaloferrocenes is readily achieved using well-established selective preparations of monolithioferrocene (FcLi, using ^tBuLi and ^tBuOK)¹⁶ and the 1,1'-dilithioferrocene-*N,N,N',N'*-tetramethylethane-1,2-diamine adduct (fcLi₂-TMEDA, using ⁿBuLi and TMEDA).¹⁷ These reactive precursors may subsequently be halogenated through combination with an appropriate (electrophilic) halide source. It should be noted that the above conditions favoring monolithiation can still provide 1,1'-dilithioferrocene in small to moderate quantities (as evidenced by the occasional observation of 1,1'-disubstitued products after quenching). In line with previous discussions,¹⁶ we suggest dilithiation can be minimized by (a) slow addition of ^tBuLi and (b) efficient stirring of the reaction mixture (both serving to reduce local heating and to avoid high local concentrations).

FcCl¹⁸ and fcCl₂^{5a} were accordingly prepared by the reaction of hexachloroethane at -78 °C with FcLi or fcLi₂-TMEDA, respectively (Scheme 1). Subsequent extraction of the crude reaction material with *n*-hexane provided mixtures of FcH and FcCl, or FcH, FcCl, and fcCl₂. These extracts were repeatedly agitated with aqueous solutions of FeCl₃ (varying their concentration, the number of washings, and the volume of oxidant solution as described in Table 1). Lower concentrations of FeCl₃ have previously been found to reduce the “oxidizing power” of the aqueous phase (and *vice versa*), in accordance with the Nernst equation.^{14c} Whereas 0.2 M FeCl₃ is sufficient to efficiently oxidize FcH ($E_{1/2} = 0.00$ V vs FcH/FcH⁺), 3.0 M FeCl₃ was required to efficiently oxidize FcCl ($E_{1/2} = 0.16$ V vs FcH/FcH⁺). (We stress that use of an inappropriate [excessive] volume or concentration of aqueous FeCl₃ for washing can readily oxidize the entire sample.) With this approach, pure FcCl and fcCl₂ (free of other ferrocene-based species) were

Table 1. Experimental Details for the Oxidative Purification of Different Haloferrocene Mixtures (FcH and FcX or FcH, FcX, and fcX₂)

compound	FcH (g) ^a	[FeCl ₃] (M)	no. of washes (mL)	pure yield	
				(g)	(%)
FcCl	4.00	0.2	2 × 200	3.03	64
FcF	0.91	0.1	3 × 50	0.32	32
fcCl ₂	9.30	3.0	3 × 200	12.7	75
fcF ₂	1.68	0.5	3 × 50	0.04	2

^aIndicative of reaction scale.

ultimately obtained following filtration of the treated solution through a pad of silica.

Preparation of fluorinated derivatives proved more challenging. We first noted established (nonexplosive/nontoxic) routes for the preparation of aryl fluorides from aryllithiums or arylmagnesium bromides.¹⁹ In our hands, however, reactions between FcLi/FcMgBr²⁰ and *N*-chloromethyl-*N'*-fluorotriethylenediammonium bis(tetrafluoroborate) (Selectfluor) or 1-fluoro-2,4,6-trimethylpyridinium triflate (FTMPT) provided no evidence of FcF. While again no FcF was observed following combination of FcMgBr and *N*-fluorobenzenesulfonimide (NFSI), the addition of NFSI to FcLi in *n*-hexane could provide pure FcF in 32% yield (following oxidative purification). Analogous conditions had been used in the preparation of 1-fluoro-2-(2-pyridyl)ferrocene,⁹ 1,2,3,4,5-pentafluoroferrocene, and FcF itself, albeit only obtained as a mixture comprising 5–20% ferrocene.⁶ We also observed the formation of 1-(phenylsulfonyl)ferrocene (among other unknown side-products), sometimes in quite significant (for example, 10% isolated) yields.

Following a similar approach, fcF₂ could be synthesized via addition of NFSI to fcLi₂-TMEDA in diethyl ether, although yields were poor and variable (typically <5%). While the material was frequently observed in crude ¹H NMR spectra, it was readily lost during workup and purification through apparent decomposition in solution or sublimation *in vacuo*. If instead, 1,1'-dilithioferrocene²¹ was prepared directly from 1,1'-dibromoferrocene^{14c} (eliminating other potentially reactive components such as TMEDA), the desired product was also observed in crude ¹H NMR spectra, but yields and purity were not improved. Reactions in *n*-hexane (instead of diethyl ether) yielded only trace quantities of product, arguably due to the reduced solubility of NFSI and fcLi₂-TMEDA in this solvent. If dimethyl ether was used (with even greater solubilizing power), the rate of reaction appeared to increase (more rapid color changes), but not the isolated yield. Future efforts toward fluorinated metallocenes might benefit from recent developments in transition-metal-catalyzed fluorinations (for example, from phenols,²² aryl triflates,²³ stannanes,²⁴ boronic acids,²⁵ silanes,²⁶ or iodides²⁷).

As with FcCl and fcCl₂, aqueous FeCl₃ was used to remove FcH and FcH/FcF impurities from FcF and fcF₂, respectively (Table 1). Yields proved highly sensitive to the number of washes, and much lower FeCl₃ concentrations had to be used compared to all other halogenated materials. This prompted further investigation of their electrochemical properties.

b. Electrochemistry. All materials were studied by solution voltammetry in MeCN/0.1 M NBu₄PF₆ and exhibited essentially reversible behavior ($i_{pa}/i_{pc} \approx 1$, $i_p \propto V_s^{1/2}$; data summarized in Table 2). A comparison of equilibrium potentials for FcX and fcX₂ shows that FcH is easier to oxidize

Table 2. Electrochemical Data^a

compound	E_{pa}/V	E_{pc}/V	$\Delta E/V^b$	i_{pa}/i_{pc}^c	$E_{1/2}/V^c$
FcF	0.063	0.134	0.071	0.99	0.098
	0.091 ^d	0.118 ^d		0.95 ^d	0.105 ^d
FcCl	0.130	0.194	0.064	1.01	0.162
FcBr	0.133	0.201	0.068	1.00	0.167
FcI	0.116	0.194	0.078	1.00	0.155
fcF ₂	0.208	0.270	0.062	1.09	0.239
fcCl ₂	0.286	0.346	0.060	0.99	0.316
fcBr ₂	0.279	0.359	0.080	1.03	0.319
fcI ₂	0.250	0.323	0.073	1.04	0.287

^aFor scan rate = 0.1 V s⁻¹. Bu₄N⁺PF₆⁻ (0.1 M) in MeCN; working electrode: glassy carbon; reference electrode, counter electrode: Pt. All potentials (error = ±0.02 V) assigned to the Fe²⁺/Fe³⁺ redox couple and reported relative to an internal FcH/FcH⁺ reference. Data from this work and ref 14c. ^b $\Delta E > 0.060$ V due to a small uncompensated solution resistance effect. ^cFrom cyclic voltammetry experiments unless otherwise stated, where $E_{1/2} = 1/2(E_{pa} + E_{pc})$. ^dFrom differential pulse voltammetry experiments, where $E_{1/2} = E_{pa/pc} \pm$ pulse height/2.

than FcX, which in turn is easier to oxidize than fcX₂ (for the same halide). This result holds true across both FcX and fcX₂ series (X = I, Br, Cl, F) and is in line with the notion that as the number of electron-withdrawing substituents on the cyclopentadienyl ring increases, the complex becomes more difficult to oxidize (the HOMO in the parent ferrocene being largely metal-centered;²⁹ also see the theoretical section). Within each series, however, we observed that FcF and fcF₂ are the complexes *easiest* to oxidize. This was surprising given that fluorine is widely considered the most electronegative of all elements³⁰ (always more electronegative than the other halides, it is actually the *second* most electronegative element, after neon, on the Allen scale³¹). Removal of electron density via inductive effects should render the Fe center more electron deficient (and so more difficult to remove an electron).³² Based on electronegativity alone, oxidation potentials following the order F > Cl > Br > I might be expected, yet in the experimental data we see Br ~ Cl > I > F (within a ~10 mV experimental error). It is apparent that no simple correlation exists between substituent electronegativity and $E_{1/2}$ in these complexes. Studies elsewhere have made similar observations: 1,2,3,4,5-pentachloroferrocene ([FeCp(C₅Cl₅)], $E^0 = 0.77$ V vs FcH/FcH⁺; reversible only at high scan rates)³³ is reportedly much more difficult to oxidize than 1,2,3,4,5-pentafluoroferrocene ([FeCp(C₅F₅)], $E_0 = 0.01$ V vs FcH/FcH⁺).⁶ [FcB(C₆Cl₅)₂] has also been observed to exhibit a higher equilibrium potential than [FcB(C₆F₅)₂] ($E_{1/2} = 0.55$ V vs 0.45 V, respectively, although the C₆Cl₅ group is in this case considered more electron withdrawing).³⁴

Several contributing factors to the ease of oxidation of fluoroferrocenes may be considered. These are discussed with reference to relevant spectroscopic and crystallographic data (see below). First we wondered if very electron-withdrawing substituents on the cyclopentadienyl anion (Cp⁻) ring might hamper its electron-donating ability, thus weakening the Cp–Fe bond and reducing the inductive electron-withdrawing effect felt at Fe. A weaker bond would, however, result in a longer Cp–Fe distance, whereas the X-ray crystal structure of [FeCp(C₅F₅)]⁶ clearly shows the (C₅F₅)–Fe bond is shorter (invalidating this theory). Likewise, any possibility of F–Fe orbital interactions—for example, agostic bonding/p orbital overlap (increasing the electron density at Fe)—appears

unlikely following the observation that the fluoride substituents are bent outward and away from the ferrocene center.

We next questioned the role resonance effects might play in stabilizing a positive charge, as increased charge delocalization would likely increase the stability of the oxidized product with respect to the reduced product in electrochemical equilibria. A useful discussion in this context was put forward by Richardson and co-workers, who observed that [Ru(C₅F₅)Cp*] was marginally easier to oxidize than [Ru(C₅Cl₅)Cp*] ($E_{pa} = 1.07$ vs 1.11 V, respectively, although in both cases the redox processes were either irreversible or quasi-reversible).³⁵ Here the authors suggested that the similar E_{pa} values in these complexes could be rationalized using empirically determined substituent constants (such as those introduced by Hammett³⁶). For Cl and F substituents the measured differences in polarizability, inductive/field effects (likely playing a negligible role here), and π resonance effects on aromatic rings were considered to largely cancel each other out. Values of the Hammett (σ_p), field/inductive (F), and resonance effect (R) parameters for the halides—compiled by Hansch, Leo, and Taft³⁷—are provided in Table 3 (generally, the more negative

Table 3. Hammett (σ_p), Field/Inductive (F), and Resonance Effect (R) Parameters for Halide Substituents³⁷

substituent	σ_p	F	R
F	0.06	0.45	-0.39
Cl	0.23	0.42	-0.19
Br	0.23	0.45	-0.22
I	0.18	0.42	-0.24

the value, the greater the stabilization of a positive charge). The biggest variations here can be seen to arise from the contributions of resonance effects, where the strong donating ability of fluorine is attributed to favorable 2p–2p F–C orbital interactions. It is interesting to note that some correlation between R for halide substituents and $E_{1/2}$ for FcX and fcX₂ can be observed (Figure 1), although deviations from the linear fit suggest resonance effects may not be the only contributing factor.

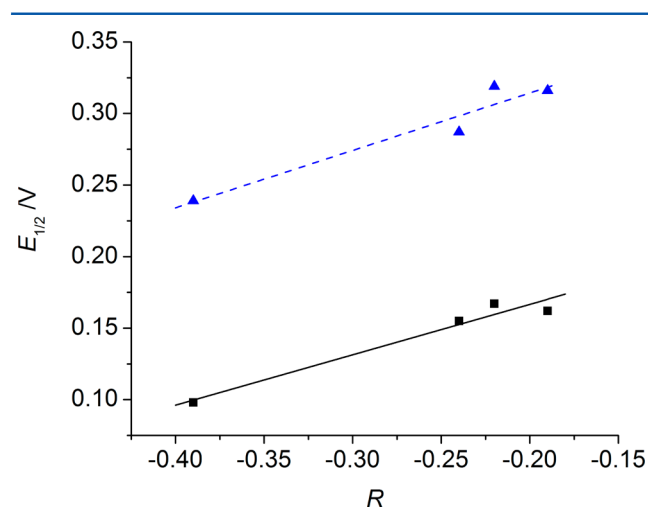


Figure 1. Resonance effect parameters (R) for halide substituents plotted against $E_{1/2}$ for FcX (black squares, solid line) and fcX₂ (blue triangles, dotted line).

Table 4. Selected ^1H and $^{13}\text{C}\{^1\text{H}\}$ NMR,^a UV–Vis,^b and IR^c Spectroscopic Data^d

compound	δ/ppm							$\lambda_{\text{max}}/\text{nm}$ ($\epsilon/\text{M}^{-1}\text{cm}^{-1}$)	Cp–X/ cm^{-1}
	H_α ^e	H_β ^e	C_3H_5	C–X	C_α	C_β	C_5H_5		
FcH			4.18				68.05	442.0 (92)	
FcF	4.31	3.79	4.26	135.76	56.18	61.15	69.44	435.5 (96)	1468
FcCl	4.39	4.05	4.24	92.46	66.14	68.00	70.39	438.4 (105)	880 ^f
FcBr	4.41	4.10	4.23	77.76	67.21	70.24	70.73	438.6 (123)	870 ^f
FcI	4.41	4.15	4.19	39.85	68.97	74.16	71.19	439.6 (162)	863 ^f 852 ^f
fcF ₂	4.39	3.90		135.87	57.47	62.53		430.9 (92)	1465
fcCl ₂	4.42	4.13		93.28	68.53	70.11		436.1 (241)	891 ^f 874 ^f
fcBr ₂	4.43	4.17		78.40	70.07	72.81		437.0 (71)	877 ^f 865 ^f
fcI ₂	4.37	4.18		40.42	72.41	77.72		440.5 (214)	864 ^f

^aIn CDCl_3 . ^bIn MeCN ($\sim 1\text{--}2\text{ mM}$). ^cATR. ^dFrom this work and refs 14c and 41. ^eAssignment based on assumption that H_α has a greater downfield shift than H_β . ^fC–X stretch combined with C–H out-of-plane bending.

Given that upon oxidation an electron is removed from the HOMO, it is important also to consider changes to the ligand and metal character of frontier orbitals in ferrocenes upon Cp substitution. Previous work by Dowben and co-workers (concerning the photoelectron spectra of methylated and halogenated 1,1'-substituted ferrocenes) suggested that the greater the charge transfer from a Cp ring to its substituent, the greater the mixing of Fe $d_{x^2-y^2,xy}$ and Cp (e_{2g}) π orbitals.³⁸ Increased mixing results in a HOMO of higher binding energy and so renders that complex more difficult to oxidize. While 1,1'-dimethylferrocene followed the anticipated trend, the authors noted that the experimentally determined HOMO (a1g) energy of **fcBr₂** (7.17 eV with respect to the vacuum level) was marginally higher than that of **fcCl₂** (7.1 eV). As Cl has a higher electronegativity than Br, it was argued (neglecting resonance effects) that in **fcCl₂** there should be greater charge transfer from the Cp ring and thus greater Fe $d_{x^2-y^2,xy}$ and Cp (e_{2g}) π mixing and a HOMO of higher binding energy (for FcH, $E(\text{a1g}) = 6.9\text{ eV}$). Interestingly, this³⁸ and similar observations⁶ have previously been attributed to experimental error. In light of the additional experimental evidence presented here (through systematic analysis of the FcX and fcX₂ series), we suggest such properties should instead be accepted and rationalized.

c. NMR, UV–Vis, and IR Spectroscopy. In contrast to electrochemical observations, spectroscopic trends largely correlate with the electronegativity of substituents (Table 4). For example, the chemical shift difference between H_α and H_β resonances increases for both the FcX and fcX₂ series as $\text{I} < \text{Br} < \text{Cl} < \text{F}$. This occurs primarily from upfield shifts of all the H_β resonances (up to 0.39 ppm from that of the parent ferrocene Cp–H signal), with nuclei actually becoming more shielded with increasing substituent electronegativity. In contrast, the H_α and unsubstituted Cp ring resonances (where relevant) move downfield (up to 0.25 and 0.08 ppm from that of the parent ferrocene Cp–H signal, respectively). In the ^1H NMR spectra of the fluorinated derivatives it is also of note that the pseudotriplets characteristic of a monosubstituted Cp ring are split further through coupling to the ^{19}F nuclei, as indeed are the resonances of carbon nuclei on fluorine-substituted Cp rings (SI, Figures S5, S6, S10, and S11). The observed $^{13}\text{C}\text{--}^{19}\text{F}$ coupling constants for fluorinated ferrocenes ($^1J_{\text{C-F}} = 265.4, 269.2\text{ Hz}$; $^2J_{\text{C-F}} = 14.9, 15.4\text{ Hz}$; $^3J_{\text{C-F}} = 3.2\text{ Hz}$) closely match those measured in fluorobenzene ($^1J_{\text{C-F}} = 245.0\text{ Hz}$; $^2J_{\text{C-F}} =$

21.1 Hz ; $^3J_{\text{C-F}} = 2.5\text{ Hz}$). Perhaps unsurprisingly, the largest chemical shift changes in $^{13}\text{C}\{^1\text{H}\}$ spectra are with nuclei of carbon atoms directly bonded to halides. These become increasingly deshielded with increasing electronegativity of the substituent, whereas the C_α and C_β nuclei become more shielded (as observed with H_α and H_β).

UV–vis spectroscopy was used to determine the optical properties of the series, where the relative energies of the HOMO–LUMO gap were of particular interest. Table 4 presents measured values of the unresolved $^1\text{A}_{1g} \rightarrow ^1\text{E}_{1g}$ and $^1\text{A}_{1g} \rightarrow ^1\text{E}_{2g}$ spin-allowed d–d transitions for each compound (occurring at 442 nm for the parent ferrocene in THF).³⁹ Here only very small differences are observed, although in each case λ_{max} increases from $\text{F} < \text{Cl} < \text{Br} < \text{I} < \text{H}$ (increasing HOMO–LUMO gap with increasing electronegativity).

The IR spectra of each compound exhibits absorptions typical of the parent ferrocene, in addition to others associated with the halogen substituents (SI, Figures S15–18 and Table S1). Sünkel et al. had previously associated peaks at 1506 and 939 cm^{-1} with the C_5F_5 ring, and we note similar features in the spectra of both mono- and dihalo derivatives (**FcF**: 1468 and 928 cm^{-1} ; **fcF₂**: 1465 and 932 cm^{-1}). With the aid of simulated spectra from first-principles calculations (see the next section for more details) all bands could be fully assigned (SI, Table S1). We find that the absorptions at 1465–1506 correspond to C–F stretching, whereas those at 928–939 cm^{-1} are attributable to C–H/F deformation. Interestingly, C–X bond stretches in halogenated ferrocenes follow the same trend in relative energies as the halobenzenes (where $\text{C–F} > \text{C–Cl} > \text{C–Br} > \text{C–I}$), yet typically occur at higher energies. For example, $\text{C–F}_{(\text{ferrocene})} = 1468\text{ cm}^{-1}$ versus $\text{C–F}_{(\text{fluorobenzene})} = 1232\text{ cm}^{-1}$ (Figures S16–17).⁴⁰

d. X-ray Crystallography. With the recent publication of a crystal structure for 1,1'-diiodoferrocene,⁴² we sought to obtain the final three structures remaining in the FcX and fcX₂ series. It was hoped structural comparisons might offer additional insights into the redox properties observed. While data for **fcF₂** (Figure 2; SI, Figure S20) and **fcCl₂** (Figure 3; SI, Figure S21) were readily obtained, attempts to get good quality data for **FcF** (SI, Figure 19) proved challenging: the structure proved to be highly disordered and thus useless for geometric analysis (see the SI for more details). Unfortunately, this situation could not be improved regardless of whether crystals were grown from *n*-hexane, EtOH, or toluene. Available experimental data are

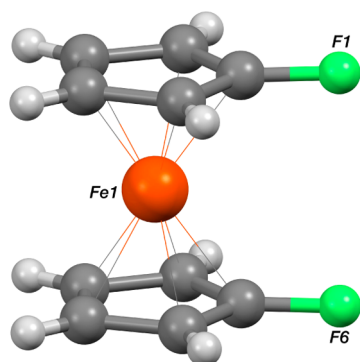


Figure 2. Crystal structure of FcF_2 .

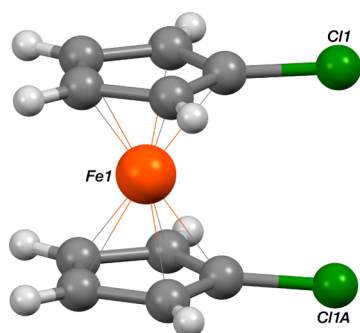


Figure 3. Crystal structure of the C_2 -symmetric complex FcCl_2 . The C_2 axis passes through the iron center and bisects the $\text{Cl1}\cdots\text{Cl1A}$ vector.

collected in Table 5, where calculated bond lengths and angles are included in square brackets for comparison. The latter are in excellent agreement with experiment and likely well-representative of the actual parameters for FcF . The anticipated increase in $\text{C}-\text{X}$ bond length with $\text{F} < \text{Cl} < \text{Br} < \text{I}$ is clear (in good agreement with IR spectroscopy). $\text{C}-\text{X}$ substituents in these metallocenes appear marginally bent away from the Fe center; distances between the Cp plane and the halogen range from 0.023 to 0.136 Å. Unfortunately, no trends in line with the electrochemical behavior are easily determined from the structural information.

We also obtained the structure of FcSO_2Ph , which was found to contain two crystallographically independent complexes, **3a-I** and **3a-II**, both shown in Figure 4 (see also SI, Figure S22).

e. First-Principles Calculations. In order to rationalize the ease with which fluorinated ferrocenes are oxidized, we have

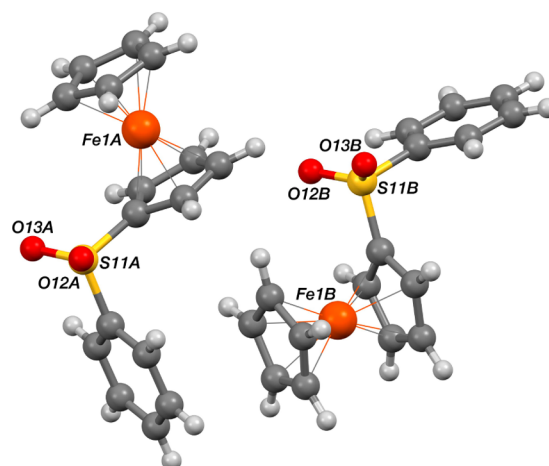


Figure 4. Crystal structure of FcSO_2Ph showing the two independent complexes $\text{FcSO}_2\text{Ph-A}$ and $\text{FcSO}_2\text{Ph-B}$.

performed density functional theory calculations. Energy levels and ionization energies have been determined for the isolated molecules and for solvated molecules using the conductor-like screening model (COSMO). All calculations have been carried out using the Turbomole program. The molecular orbitals are expanded in an atom-centered Gaussian basis set of TZVPP quality,⁴⁷ electronic exchange and correlation are described by the B3LYP hybrid-exchange functional, and the D2 correction of Grimme is used to describe long-range London dispersion interactions.⁴⁸

It is not unreasonable to expect that substitution with an electronegative element should make ferrocene more difficult to oxidize. This expectation is based on a simple model; as the HOMO in ferrocene is largely metal-centered and expected to be of a_{1g} character,^{29b} the withdrawal of electrons from the ferrocene ring by electronegative substitution reduces Coulomb repulsion between the HOMO and the ring. The degree of stabilization is thus expected to be directly related to the electronegativity of the substituent. This trend has been observed, for example, in studies on fluorinated syndones by Oshima et al.⁴⁹

The computed HOMO eigenvalues in the first column of Table 6 show that the monofluorination of ferrocene stabilizes the HOMO as expected (by 0.29 eV). The monosubstitution of Cl, Br, or I produces further stabilization (0.35, 0.38, and 0.37 eV). This is consistent with the observed trend in the cyclic

Table 5. Selected Structural Parameters^a

compound	$r_{\text{C-X}}$	$r_{\text{CpX}_{n-1}\text{-Fe}}$ ^b	$r_{\text{Cp-Fe}}$ ^b	$r_{\text{Cp(plane)-X}}$ ^c	ref
FcH			1.661, 1.655 [1.669]		43
FcF	[1.344]	[1.666]	[1.669]	[0.026]	this work
FcCl	1.708(7), 1.733(5) [1.735]	1.641, 1.642 [1.664]	1.648, 1.664 [1.669]	0.076, 0.102 [0.055]	44
FcBr	1.882(2), 1.894(2) [1.898]	1.640, 1.645 [1.663]	1.651, 1.657 [1.668]	0.041, 0.082 [0.058]	44
FcI	2.085(5), 2.088(5) [2.095]	1.643, 1.648 [1.662]	1.652, 1.653 [1.669]	0.068, 0.088 [0.053]	45
FcF_2	1.357(3) [1.343]	1.6514(12), 1.6519(12) [1.666]		0.044 [0.018]	this work
FcCl_2	1.724(2) [1.734]	1.6486(8) [1.665]		0.091 [0.048, 0.049]	this work
FcBr_2	1.866(4), 1.882(4) [1.896]	1.648, 1.650 [1.664]		0.082, 0.136 [0.050]	46
FcI_2	2.0838(1)–2.0940(1) [2.095]	1.636–1.646 [1.662]		0.023–0.048 [0.040, 0.041]	42
$[\text{FcCp}(\text{C}_5\text{F}_5)]$	1.331(2)–1.341(3) [1.333]	1.602 [1.624]	1.657 [1.675]	0.073–0.091 [0.054–0.057]	6

^aExperimental bond lengths (in Å), where available. Data in square brackets were obtained from first-principles calculations. If multiple, nonidentical distances were found, minimum and maximum values are provided to give an indication of the range. ^b $r_{\text{CpX}_{n-1}\text{-Fe}}$ = Fe-substituted Cp centroid distance. $r_{\text{Cp-Fe}}$ = Fe–Cp centroid distance. ^cThe distance between the Cp plane and X.

Table 6. HOMO and Ionization Energies (IE) of Halogenated Ferrocenes (TZVPP, B3LYP, COSMO for Acetonitrile⁵⁰)

compound	HOMO/eV ^a	HOMO/eV ^b	IE/eV ^a	IE/eV ^b
FcH	-5.29	-5.45	6.32	4.52
FcF	-5.58	-5.55	6.45	4.60
FcCl	-5.64	-5.58	6.46	4.67
FcBr	-5.67	-5.59	6.47	4.69
FcI	-5.66	-5.56	6.46	4.68
fcF ₂	-5.75			
fcCl ₂	-5.85			
fcBr ₂	-5.89			
fcI ₂	-5.86			
[FeCp(C ₃ F ₃)]	-6.36		7.15	
[Fe(C ₃ F ₃) ₂]	-7.11		7.82	

^aAfter optimization. ^bAfter optimization with COSMO.

voltammetry measurements described above and suggests that electronegativity is not the dominant factor influencing oxidation. DFT eigenvalues of the isolated molecules are only a guide to the ionization energy (IE). The same trend is, however, maintained for the IE computed as the energy difference between the molecule and the positive ion (column 3 in Table 6). The trend is also preserved when the screening of the solvent is included using the COSMO approximation (columns 2 and 4 of Table 6).

Insight into the interaction affecting the HOMO energy can be gained by examining the computed electronic structure. Molecular orbital diagrams for ferrocene typically propose a LUMO of e_{1g} symmetry (d_{xz} and d_{yz} orbitals), a HOMO of a_{1g} symmetry (d_z^2 orbitals), and a HOMO-1 of e_{2g} symmetry ($d_{x^2-y^2}$ and d_{xy} orbitals).^{29b} This is not, however, the picture that emerges from our DFT calculations. In the computed molecular orbitals the HOMO is composed predominantly of e_{2g} ($d_{x^2-y^2}$, d_{yx}) atomic orbitals and not of the a_{1g} (d_z^2) orbitals. In contrast to the a_{1g} (d_z^2) orbitals, the e_{2g} ($d_{x^2-y^2}$, d_{yx}) atomic orbitals lie planar to the Cp rings. The energy of the HOMO is thus influenced by a combination of electrostatic repulsion and the hybridization of the planar $d_{x^2-y^2}$ and d_{yx} orbitals with the Cp ring orbitals. Withdrawal of electrons from the ring by electronegative substitution reduces hybridization and thus destabilizes the HOMO. The position of the HOMO is determined by a balance between the competing influence of changes in electrostatic repulsion and covalent stabilization. Cl, Br, and I are less electronegative than F, and therefore monosubstitution with these elements leads to less reduction of the covalent stabilization. Consequently, in comparison to monofluorination, the HOMO is further stabilized (columns 2 and 3 of Table 6).

The molecular orbital compositions and bond orders give further insight into the stabilization mechanism (Tables 7 and 8). The molecular orbital compositions show that the HOMO becomes less metal-centered upon halogenation (column 2 of Table 7), thus showing reduced electrostatic repulsion. The monofluorination of ferrocene leads to the least metal-centered HOMO (column 2 of Table 7). It is only for monoiodinated ferrocene that the halogen atom gives a significant contribution to the HOMO and HOMO-1 orbitals (column 5 of Table 7). It appears that the greater polarizability of iodine leads to an enhanced hybridization with the metal center. In particular, monofluorinated and monoiodinated ferrocene show significant contributions of the Cp rings to the HOMO (column 3 of

Table 7. Molecular Orbital Compositions for Halogenated Ferrocenes (TZVPP, B3LYP, HOMO: e_{2g} ; HOMO-1: a_{1g})

compound	HOMO (HOMO-1)/%			
	Fe	C	H	X
FcH	85.5 (91)	14 (6)	0.5 (3)	
FcF	76.5 (87)	22.5 (9)	0.5 (3)	0.5 (1)
FcCl	80 (88)	18 (8)	0.5 (3)	1.5 (1)
FcBr	79.5 (82)	17.5 (10)	0.5 (3)	2 (5)
FcI	77.5 (42)	19 (23)	0 (2)	4 (33)

Table 8. Bond Orders for Fe-Cp (TZVPP, B3LYP)

compound	Fe-Cp bond order
FcH	1.976
FcF	2.070
FcCl	2.074
FcBr	2.076
FcI	2.065

Table 7). This can be attributed to π -resonance effects of the aromatic system and is in accordance with the experimental observation that fluorine and iodine show the highest resonance effects of all halide substituents (column 4 of Table 3). The computed bond orders also reflect changes in covalent stabilization; the monoiodinated and -fluorinated ferrocenes have lower bond orders than the other haloferrocenes (column 2, Table 8).

In addition to the electrostatic repulsion and covalent stabilization the size and polarizability of the halogens may also affect the IE. Withdrawal of electrons from the ring by electronegative substitution increases the electrostatic through-space repulsion between the halogen atom and the iron center. Solvent molecules may screen this interaction. However, with increasing halogen size, this screening effect is minimized through steric hindrance of the screening molecules. Therefore, the size of the halogen also influences the balance between electrostatic through-space repulsion and covalent stabilization. As a consequence, in comparison to monochlorination, monobromination makes oxidation harder to achieve (column 6 of Table 2; columns 4 and 5 of Table 6). This model successfully accounts for the trends in both the mono- and bihalogenated ferrocenes. The HOMO energies of the bihalogenated ferrocenes show the same trend as the HOMO energies of the monohalogenated ferrocenes (column 2 of Table 6). However, in comparison to the monohalogenated ferrocenes, the HOMO energies of the bihalogenated ferrocenes are marginally lower, thus generally showing a higher stabilization. This is in accordance with the experimental observation that the bihalogenated ferrocenes are generally harder to oxidize than the monohalogenated ferrocenes (column 5 of Table 2).

The experimental observation that pentafluorination further reduces the IE is not consistent with this model or with the computed IE (column 2 of Table 6). This observation has, however, been reported in a single publication⁶ and needs further verification.

CONCLUSION

All of the halo and 1,1'-dihaloferrocenes (X = I, Br, Cl, F) have now been prepared and characterized within a single laboratory. In contrast to the findings of previous studies, we demonstrate that all these materials may be obtained in high purity using

straightforward, readily available methods such as oxidative purification (here extended to Cl and F derivatives) and column chromatography. With this approach it proves possible to separate compounds with only ~ 100 mV differences in $E_{1/2}$ (for example, FcH and FcF). Solution voltammetry and first-principle studies confirm the perhaps counterintuitive result that ferrocenes with increasingly electron-withdrawing substituents become first harder, then easier to oxidize. A theoretical model, which explains the observed trends, has been introduced. In the quest for high-oxidation-resistant metallocenes this work has important ramifications, not least suggesting that the most difficult to oxidize perhaloferrocenes have already been prepared (decachloroferrocene^{11b,13} and decabromoferrocene⁵¹).

EXPERIMENTAL SECTION

General Considerations. All reactions were performed under an atmosphere of nitrogen. Solvents used in reactions were sparged with nitrogen and dried with alumina beads or Q5 copper catalyst on molecular sieves, where appropriate. Mass spectrometry analyses were conducted by the Mass Spectrometry Service, Imperial College London. ^1H , $^{13}\text{C}\{^1\text{H}\}$, and $^{19}\text{F}\{^1\text{H}\}$ NMR were recorded on a Bruker 400 MHz spectrometer and referenced to the residual solvent peaks of CDCl_3 at 7.26 and 77.16 ppm or externally to 85% phosphoric acid (0.00 ppm), respectively. UV-vis and IR spectra were recorded on a PerkinElmer LAMBDA 25 UV/vis spectrophotometer or a PerkinElmer Spectrum 100 FT-IR spectrometer, respectively. Microanalyses were carried out by Stephen Boyer of the Science Centre, London Metropolitan University. FcI, FcBr, fcI₂, and fcBr₂ were prepared using literature procedures or purchased from Sigma-Aldrich, UK.^{14c} All other reagents were commercially available and used as received.

Cyclic voltammograms were recorded under an atmosphere of argon in MeCN/0.1 M $^n\text{Bu}_4\text{NPF}_6$ on a CHI760C potentiostat (CH Instruments, Austin, TX, USA) with a glassy carbon disc as working electrode (diameter = 2.5 mm) and Pt wire as reference and counter electrodes, respectively. Analyte solutions were between 0.1 and 1 mM. Potentials are reported relative to an internal $[\text{FcH}]^+ / [\text{FcH}]$ reference.

Chloroferrocene (FcCl).¹⁸ A mixture of ferrocene (4.00 g, 21.5 mmol, 1 equiv), potassium *tert*-butoxide (0.03 g, 2.68 mmol, 0.12 equiv), and THF (120 mL) was stirred in an oven-dried 250 mL three-necked flask and cooled to -78 °C (acetone/dry ice). $^t\text{BuLi}$ (1.9 M) in pentane (23 mL, 43.2 mmol, 2 equiv) was added dropwise, and the mixture vigorously stirred for 2 h. To the resulting orange suspension was added hexachloroethane (7.65 g, 32.3 mmol, 1.5 equiv) portionwise against nitrogen. After stirring for a further 30 min at -78 °C, the mixture was allowed to warm slowly to ambient temperature by not adding dry ice. The dark orange solution was then carefully quenched with water (~ 10 mL) and extracted with CH_2Cl_2 , and solvent was removed.

The crude product was extracted into *n*-hexane (~ 300 mL) and washed with 0.2 M aqueous FeCl_3 (2×200 mL). When FcH had been removed (composition monitored by ^1H NMR spectroscopy between washings), the organic phase was extracted with water until the washings were colorless, dried over MgSO_4 , and filtered (50 g silica/*n*-hexane). The solution was dried *in vacuo* to yield pure FcCl as an orange crystalline solid (3.03 g, 64%). ^1H NMR (400 MHz, CDCl_3): δ (ppm) 4.05 (pseudo-t, 2H, Cp-H, $J_{\text{HH}} = 1.83$ and 1.85 Hz), 4.24 (s, 5H, Cp-H), 4.39 (pseudo-t, 2H, Cp-H, $J_{\text{HH}} = 1.89$ and 1.90 Hz). $^{13}\text{C}\{^1\text{H}\}$ NMR (101 MHz, CDCl_3): δ (ppm) 66.14 (2C, Cp-Cl, CH), 68.00 (2C, Cp-Cl, CH), 70.39 (5C, Cp, CH), 92.46 (1C, Cp-Cl, CCl). HR-MS EI+: m/z 219.9735 ($[\text{M}]^+$ calcd 219.9742). Anal. Found: C, 54.39; H, 4.13. Calcd for $\text{C}_{10}\text{H}_9\text{FeCl}$: C, 54.45; H, 4.12.

Fluoroferrocene (FcF)^{14,6-8} and **1-(Phenylsulfonyl)ferrocene (FcSO₂Ph)**⁵² A mixture of ferrocene (0.911 g, 4.90 mmol, 1 equiv), potassium *tert*-butoxide (0.067 g, 0.60 mmol, 0.12 equiv), and THF (15 mL) was stirred in an oven-dried flask and cooled to -78 °C (acetone/dry ice). $^t\text{BuLi}$ (1.7 M) in pentane (5.8 mL, 9.86 mmol, 2

equiv) was added dropwise over ~ 20 min, and the mixture vigorously stirred for 2 h. To the resulting orange suspension was added *N*-fluorobenzenesulfonimide (2.288 g, 7.26 mmol, 1.5 equiv) portionwise against nitrogen (NOTE: effervescent reaction may result). After stirring for a further 30 min at -78 °C, the mixture was allowed to warm slowly to ambient temperature overnight by not adding dry ice. The yellow-brown suspension was then carefully quenched with water (10 mL) and filtered through Celite using CH_2Cl_2 . The solution was washed with water (1×40 mL), and the aqueous phase extracted with CH_2Cl_2 (2×25 mL). The combined organic layers were dried over MgSO_4 and filtered through Celite, and solvent was removed.

Solid material was dissolved in CH_2Cl_2 (~ 100 mL) and washed with 0.1 M aqueous FeCl_3 (3×50 mL). When FcH had been removed (composition monitored by ^1H NMR spectroscopy between washings), the organic phase was extracted with water until the washings were colorless, dried over MgSO_4 , and filtered through Celite. The residue was preabsorbed on silica and purified by column chromatography (silica; *n*-hexane \rightarrow CH_2Cl_2 /*n*-hexane [3:1]). Combined fractions from the first yellow band (eluting with *n*-hexane) yielded FcF as a light yellow solid after solvent removal (0.316 g, 32%). ^1H NMR (400 MHz, CDCl_3): δ (ppm) 3.79 (d pseudo-t, 2H, Cp-H, $J_{\text{HF}} = 1.47$ Hz), 4.26 (s, 5H, Cp-H), 4.30 (d pseudo-t, 2H, Cp-H, $J_{\text{HF}} = 2.72$ Hz, $J_{\text{HH}} = \sim 2.04$ and ~ 2.05 Hz). $^{13}\text{C}\{^1\text{H}\}$ NMR (101 MHz, CDCl_3): δ (ppm) 56.18 (d, 2C, Cp-F, CH_w , $J_{\text{C-F}} = 15.4$ Hz), 61.15 (d, 2C, Cp-F, CH_β , $J_{\text{C-F}} = 3.2$ Hz), 69.44 (s, 5C, Cp, CH), 135.76 (d, 1C, Cp-F, CF, $J_{\text{C-F}} = 265.4$ Hz). $^{19}\text{F}\{^1\text{H}\}$ NMR (377 MHz, CDCl_3): δ (ppm) -188.8 (s, Cp-F). HR-MS EI+: m/z 204.0051 ($[\text{M}]^+$ calcd 204.0038). Anal. Found: C, 58.72; H, 4.35. Calcd for $\text{C}_{10}\text{H}_9\text{FeF}$: C, 58.85; H, 4.45.

Additional colored bands were observed with increasing proportion of CH_2Cl_2 in the eluent, with some fractions identified as comprising pure 1-(phenylsulfonyl)ferrocene ($R_f = 0.24$; silica, CH_2Cl_2 /*n*-hexane [8:2]). This was isolated as an orange crystalline solid after solvent removal (0.156 g, 10%). Crystals suitable for X-ray diffraction were formed through slow evaporation of a CH_2Cl_2 /*n*-pentane solution. ^1H NMR (400 MHz, CDCl_3): δ (ppm) 4.40 (br pseudo-t, 2H, Cp-H), 4.49 (s, 5H, Cp-H), 4.68 (br pseudo-t, 2H, Cp-H), 7.40–7.54 (m, 3H, Ph-H), 7.84 (d, 2H, Ph-H, $J = 7.82$ Hz). $^{13}\text{C}\{^1\text{H}\}$ NMR (101 MHz, CDCl_3): δ (ppm) 69.39 (2C, Cp-R, CH), 70.89 (5C, Cp, CH), 71.28 (2C, Cp-R, CH), 90.37 (1C, Cp-R, CR), 126.81 (2C, Ph-R, CH_o), 129.13 (2C, Ph-R, CH_m), 132.68 (1C, Ph-R, CH_p), 143.21 (1C, Ph-R, CR). HR-MS EI+: m/z 326.0073 ($[\text{M}]^+$ calcd for $\text{C}_{16}\text{H}_{14}\text{FeO}_2\text{S}$ 326.0064).

1,1'-Dichloroferrocene (fcCl₂)^{5a} A mixture of ferrocene (9.30 g, 50 mmol, 1 equiv), TMEDA (18 mL, 125 mmol, 2.5 equiv), and *n*-hexane (60 mL) was stirred in an oven-dried 250 mL three-necked flask and cooled to 0 °C (ice-bath). $^n\text{BuLi}$ (2.5 M) in hexanes (44 mL, 110.0 mmol, 2.2 equiv) was added portionwise, and the mixture slowly raised to ambient temperature with stirring overnight. The resulting bright orange suspension (1,1'-dilithioferrocene/TMEDA) was cooled to -78 °C (acetone/dry ice), whereby hexachloroethane (26.0 g, 110 mmol, 2.2 equiv) was added over ~ 2 min against nitrogen. The reaction mixture was allowed to warm slowly to ambient temperature by not adding dry ice and stirred overnight, whereby it was quenched with water (~ 20 mL) and extracted with diethyl ether. Combined extracts were dried *in vacuo*.

The crude product was extracted into *n*-hexane (~ 300 mL), filtered through Celite, and washed successively with 3.0 M aqueous FeCl_3 (3×200 mL). When FcH and FcCl contaminants had been removed (composition monitored by ^1H NMR spectroscopy between washings), the organic phase was extracted with water until the washings were colorless, dried over MgSO_4 , and filtered (50 g silica/*n*-hexane). The solution was dried *in vacuo* to yield pure fcCl₂ as a yellow solid (12.7 g, 75%). Crystals suitable for X-ray diffraction were grown by cooling a concentrated *n*-hexane solution (from ~ 20 to 5 °C). ^1H NMR (400 MHz, CDCl_3): δ (ppm) 4.13 (pseudo-t, 4H, Cp-H, $J_{\text{HH}} = 1.96$ and 2.28 Hz), 4.42 (pseudo-t, 4H, Cp-H, $J_{\text{HH}} = 2.03$ and 2.13 Hz). $^{13}\text{C}\{^1\text{H}\}$ NMR (101 MHz, CDCl_3): δ (ppm) 68.53 (4C, Cp, CH), 70.11 (4C, Cp, CH), 93.28 (2C, Cp, CCl). HR-MS EI

+; m/z 253.9367 ($[M]^+$ calcd 253.9362). Anal. Found: C, 47.17; H, 3.23. Calcd for $C_{10}H_8FeCl_2$: C, 47.09; H, 3.16.

1,1'-Difluorofluorene (fcF₂).^{5b} A mixture of ferrocene (1.678 g, 9.02 mmol, 1 equiv), TMEDA (3.4 mL, 22.68 mmol, 2.5 equiv), and *n*-hexane (8.5 mL) was stirred in an oven-dried flask and cooled to 0 °C (ice-bath). ⁿBuLi (2.5 M) in hexanes (7.9 mL, 19.75 mmol, 2.2 equiv) was added portionwise, and the mixture slowly raised to ambient temperature with stirring overnight. (NOTE: the remaining steps were completed within the same day to minimize product decomposition.) The resulting bright orange suspension (1,1'-dilithioferrocene/TMEDA) was isolated by cannula filtration, resuspended in diethyl ether (22 mL), and cooled to -78 °C (acetone/dry ice), whereby *N*-fluorobenzene sulfonamide (6.257 g, 19.84 mmol, 2.2 equiv) was added over ~2 min against nitrogen. The reaction mixture was stirred below -70 °C for 3 h, then allowed to warm slowly to ambient temperature by not adding dry ice. After ~15 min at room temperature the yellow suspension darkened with formation of a precipitate. This mixture was cooled in an ice-bath and quenched with water (4 mL). Extraction with diethyl ether and *n*-hexane and filtration through alumina (Brockman grade II) provided a dark orange solution.

After reducing the solution in volume to ~200 mL, it was washed with 0.5 M aqueous FeCl₃ (3 × 50 mL). When FcH and FcF contaminants had been removed (composition monitored with ¹H NMR between washings), the organic phase was extracted with water until the washings were colorless and reduced in volume to <5 mL. The crude product was purified using column chromatography (silica; *n*-pentane), collecting the first yellow band. The majority of solvent was carefully removed under reduced pressure (NOTE: fcF₂ is readily sublimed *in vacuo*), then a concentrated solution was further dried in air to yield fcF₂ as an orange-yellow crystalline solid (0.041 g, 2%). Crystals suitable for X-ray diffraction were grown by slow evaporation of an *n*-hexane solution. ¹H NMR (400 MHz, CDCl₃): δ (ppm) 3.90 (d pseudo-t, 4H, Cp-H, $J_{HF} = 1.20$ Hz), 4.39 (d pseudo-t, 4H, Cp-H, $J_{HF} = 2.20$ Hz, $J_{HH} = \sim 2.18$ and ~ 2.27 Hz). ¹³C{¹H} NMR (126 MHz, CDCl₃): δ (ppm) 57.47 (d, 4C, Cp-F, CH_w , $J_{CF} = 14.9$ Hz), 62.53 (br s, 4C, Cp, CH_β), 135.9 (d, 2C, Cp-F, CF, $J_{CF} = 269.2$ Hz). ¹⁹F{¹H} NMR (377 MHz, CDCl₃): δ (ppm) -188.0 (s, 2F, Cp-F). HR-MS ES+: m/z 221.9949 ($[M]^+$ calcd 221.9943). Anal. Found: C, 54.15; H, 3.60. Calcd for $C_{10}H_8FeF_2$: C, 54.08; H, 3.63.

■ ASSOCIATED CONTENT

Supporting Information

The Supporting Information is available free of charge on the ACS Publications website at DOI: 10.1021/acs.organo- met.5b00811.

Experimental details, NMR, UV-vis, and IR spectra, additional electrochemical and crystallographic information (PDF)

Crystallographic data (CIF)

■ AUTHOR INFORMATION

Corresponding Authors

*E-mail: t.albrecht@imperial.ac.uk.

*E-mail: n.long@imperial.ac.uk.

Author Contributions

[§]M. S. Inkpen and S. Du contributed equally to this work.

Notes

The authors declare no competing financial interest.

■ ACKNOWLEDGMENTS

The authors thank Dr. Ian Butler (Bangor University, UK) for useful discussions. S.D. thanks the China Scholarship Council, and M.S.L., T.A., and N.J.L. thank the Leverhulme Trust (RPG 2012-754) for funding. M.H. and N.M.H. would like to acknowledge the use of the EPSRC UK National Service for

Computational Chemistry Software (NSCCS) at Imperial College London in carrying out this work.

■ REFERENCES

- (1) (a) Kealy, T. J.; Pauson, P. L. *Nature* **1951**, *168*, 1039. (b) Nesmeyanov, A. N.; Perevalova, E. G.; Nesmeyanova, O. A. *Dokl. Akad. Nauk SSSR* **1955**, *100*, 1099. (c) Nesmeyanov, A. N.; Sazonova, V. A.; Drozd, V. N. *Dokl. Akad. Nauk SSSR* **1959**, *126*, 1004. (d) Hedberg, F. L.; Rosenberg, H. *J. Organomet. Chem.* **1971**, *28*, C14.
- (2) (a) Atkinson, R. C. J.; Gibson, V. C.; Long, N. J. *Chem. Soc. Rev.* **2004**, *33*, 313. (b) Butler, I. R. *Eur. J. Inorg. Chem.* **2012**, *2012*, 4387.
- (3) (a) Morisaki, Y.; Chujo, Y. *Macromolecules* **2003**, *36*, 9319. (b) Xue, W.-M.; Kühn, Fritz, E.; Herdtweck, E.; Li, Q. *Eur. J. Inorg. Chem.* **2001**, *2001*, 213. (c) Sanechika, K.; Yamamoto, T.; Yamamoto, A. *Polym. J.* **1981**, *13*, 255.
- (4) (a) Engrakul, C.; Sita, L. R. *Nano Lett.* **2001**, *1*, 541. (b) Chawdhury, N.; Long, N. J.; Mahon, M. F.; Ooi, L.-I.; Raithby, P. R.; Rooke, S.; White, A. J. P.; Williams, D. J.; Younus, M. J. *Organomet. Chem.* **2004**, *689*, 840. (c) Vollmann, M.; Butenschon, H. *C. R. Chim.* **2005**, *8*, 1282. (d) Getty, S. A.; Engrakul, C.; Wang, L.; Liu, R.; Ke, S.-H.; Baranger, H. U.; Yang, W.; Fuhrer, M. S.; Sita, L. R. *Phys. Rev. B: Condens. Matter Mater. Phys.* **2005**, *71*, 241401. (e) Klein, A.; Lavastre, O.; Fiedler, J. *Organometallics* **2006**, *25*, 635. (f) Ma, J.; Vollmann, M.; Menzel, H.; Pohle, S.; Butenschon, H. *J. Inorg. Organomet. Polym. Mater.* **2008**, *18*, 41. (g) Engrakul, C.; Sita, L. R. *Organometallics* **2008**, *27*, 927. (h) Fan, Y.; Liu, I. P.-C.; Fanwick, P. E.; Ren, T. *Organometallics* **2009**, *28*, 3959. (i) Baumgardt, I.; Butenschon, H. *Eur. J. Inorg. Chem.* **2010**, *2010*, 1076. (j) Lu, Q.; Wang, X.-H.; Wang, F.-S. *Chin. J. Appl. Chem.* **2011**, *28*, 136. (k) Inkpen, M. S.; Albrecht, T.; Long, N. J. *Organometallics* **2013**, *32*, 6053. (l) Inkpen, M. S.; White, A. J. P.; Albrecht, T.; Long, N. J. *Dalton Trans.* **2014**, *43*, 15287.
- (5) (a) Kovar, R. F.; Rausch, M. D.; Rosenberg, H. *Organomet. Chem. Synth.* **1971**, *1*, 173. (b) Gren, C. K. Vanderbilt University, 2009.
- (6) Stinkel, K.; Weigand, S.; Hoffmann, A.; Blomeyer, S.; Reuter, C. G.; Vishnevskiy, Y. V.; Mitzel, N. W. *J. Am. Chem. Soc.* **2015**, *137*, 126.
- (7) (a) Peet, J. H. J.; Rockett, B. W. *J. Organomet. Chem.* **1974**, *82*, C57. (b) Adcock, W.; Khor, T. C. *J. Organomet. Chem.* **1975**, *91*, C20.
- (8) Popov, V. I.; Lib, M.; Haas, A. *Ukr. Khim. Zh. (Russ. Ed.)* **1990**, *56*, 1115.
- (9) Stinkel, K.; Weigand, S. *Inorg. Chim. Acta* **2011**, *370*, 224.
- (10) (a) Curnow, O. J.; Hughes, R. P. *J. Am. Chem. Soc.* **1992**, *114*, 5895. (b) Hughes, R. P.; Zheng, X.; Ostrander, R. L.; Rheingold, A. L. *Organometallics* **1994**, *13*, 1567. (c) Hughes, R. P.; Zheng, X.; Morse, C. A.; Curnow, O. J.; Lompfrey, J. R.; Rheingold, A. L.; Yap, G. P. A. *Organometallics* **1998**, *17*, 457.
- (11) (a) Winter, C. H. Synthesis and Properties of Perfluorofluorene and Perfluororuthenocene. A Potential Class of High Temperature Materials; Dept. Chem., Wayne State Univ., Detroit, MI, USA, 1995. (b) Hedberg, F. L.; Rosenberg, H. *J. Am. Chem. Soc.* **1973**, *95*, 870.
- (12) Koplitz, L. V.; McClure, D. S.; Crerar, D. A. *Inorg. Chem.* **1987**, *26*, 308.
- (13) (a) Hedberg, F. L.; Rosenberg, H. *Oxidation-resistant metal-locenes. The synthesis and properties of perchloroferrocene and related polychlorinated and fluorinated ferrocenes*; Air Force Materials Laboratory, Wright-Patterson Air Force Base, OH, 1970. (b) Hedberg, F. L.; Rosenberg, H. *J. Am. Chem. Soc.* **1970**, *92*, 3239.
- (14) (a) Cunningham, K. L.; McMillin, D. R. *Polyhedron* **1996**, *15*, 1673. (b) Goeltz, J. C.; Kubiak, C. P. *Organometallics* **2011**, *30*, 3908. (c) Inkpen, M. S.; Du, S.; Driver, M.; Albrecht, T.; Long, N. J. *Dalton Trans.* **2013**, *42*, 2813.
- (15) Bulfield, D.; Maschke, M.; Lieb, M.; Metzler-Nolte, N. *J. Organomet. Chem.* **2015**, *797*, 125.
- (16) Sanders, R.; Mueller-Westerhoff, U. T. *J. Organomet. Chem.* **1996**, *512*, 219.
- (17) (a) Rausch, M. D.; Ciappenelli, D. J. *J. Organomet. Chem.* **1967**, *10*, 127. (b) Bishop, J. J.; Davison, A.; Katcher, M. L.; Lichtenberg, D. W.; Merrill, R. E.; Smart, J. C. *J. Organomet. Chem.* **1971**, *27*, 241.

- (c) Butler, I. R.; Cullen, W. R.; Ni, J.; Rettig, S. J. *Organometallics* **1985**, *4*, 2196.
- (18) Bernhartzeder, S.; Sünkel, K. J. *Organomet. Chem.* **2012**, *716*, 146.
- (19) (a) Davis, F. A.; Han, W.; Murphy, C. K. *J. Org. Chem.* **1995**, *60*, 4730. (b) Snieckus, V.; Beaulieu, F.; Mohri, K.; Han, W.; Murphy, C. K.; Davis, F. A. *Tetrahedron Lett.* **1994**, *35*, 3465. (c) Umemoto, T.; Fukami, S.; Tomizawa, G.; Harasawa, K.; Kawada, K.; Tomita, K. *J. Am. Chem. Soc.* **1990**, *112*, 8563. (d) Yamada, S.; Knochel, P. *Synthesis* **2010**, *2010*, 2490. (e) Yamada, S.; Gavryushin, A.; Knochel, P. *Angew. Chem., Int. Ed.* **2010**, *49*, 2215.
- (20) Shechter, H.; Helling, J. F. *J. Org. Chem.* **1961**, *26*, 1034.
- (21) U.S. Patent 3,422,129 A, 1969.
- (22) Tang, P.; Wang, W.; Ritter, T. *J. Am. Chem. Soc.* **2011**, *133*, 11482.
- (23) Watson, D. A.; Su, M.; Teverovskiy, G.; Zhang, Y.; García-Fortanet, J.; Kinzel, T.; Buchwald, S. L. *Science* **2009**, *325*, 1661.
- (24) (a) Furuya, T.; Strom, A. E.; Ritter, T. *J. Am. Chem. Soc.* **2009**, *131*, 1662. (b) Tang, P.; Furuya, T.; Ritter, T. *J. Am. Chem. Soc.* **2010**, *132*, 12150.
- (25) (a) Furuya, T.; Kaiser, H. M.; Ritter, T. *Angew. Chem., Int. Ed.* **2008**, *47*, 5993. (b) Furuya, T.; Ritter, T. *Org. Lett.* **2009**, *11*, 2860.
- (26) Tang, P.; Ritter, T. *Tetrahedron* **2011**, *67*, 4449.
- (27) Fier, P. S.; Hartwig, J. F. *J. Am. Chem. Soc.* **2012**, *134*, 10795.
- (28) Furuya, T.; Kamlet, A. S.; Ritter, T. *Nature* **2011**, *473*, 470.
- (29) (a) Haaland, A. *Acc. Chem. Res.* **1979**, *12*, 415. (b) Long, N. J. *Metalloenes: Introduction to Sandwich Complexes*; Wiley-Blackwell, 1997.
- (30) (a) Pauling, L. *The Nature of the Chemical Bond*, 3rd ed.; Cornell University Press, 1960. (b) *CRC Handbook of Chemistry and Physics*, 95th ed.; CRC Press: United States, 2014–2015.
- (31) Allen, L. C. *J. Am. Chem. Soc.* **1989**, *111*, 9003.
- (32) Roemer, M.; Heinrich, D.; Kang, Y. K.; Chung, Y. K.; Lentz, D. *Organometallics* **2012**, *31*, 1500.
- (33) Brown, K. N.; Gulyas, P. T.; Lay, P. A.; McAlpine, N. S.; Masters, A. F.; Phillips, L. *J. Chem. Soc., Dalton Trans.* **1993**, 835.
- (34) (a) Kelly, M. J.; Tirfoin, R.; Gilbert, J.; Aldridge, S. *J. Organomet. Chem.* **2014**, *769*, 11. (b) Ashley, A. E.; Herrington, T. J.; Wildgoose, G. G.; Zaher, H.; Thompson, A. L.; Rees, N. H.; Krämer, T.; O'Hare, D. *J. Am. Chem. Soc.* **2011**, *133*, 14727.
- (35) Richardson, D. E.; Ryan, M. F.; Geiger, W. E.; Chin, T. T.; Hughes, R. P.; Curnow, O. J. *Organometallics* **1993**, *12*, 613.
- (36) (a) Hammett, L. P. *Chem. Rev.* **1935**, *17*, 125. (b) Hammett, L. P. *J. Am. Chem. Soc.* **1937**, *59*, 96.
- (37) Hansch, C.; Leo, A.; Taft, R. W. *Chem. Rev.* **1991**, *91*, 165.
- (38) Dowben, P. A.; Driscoll, D. C.; Tate, R. S.; Boag, N. M. *Organometallics* **1988**, *7*, 305.
- (39) (a) Gray, H. B.; Sohn, Y. S.; Hendrickson, N. *J. Am. Chem. Soc.* **1971**, *93*, 3603. (b) Rösch, N.; Johnson, K. H. *Chem. Phys. Lett.* **1974**, *24*, 179. (c) Yamaguchi, Y.; Ding, W.; Sanderson, C. T.; Borden, M. L.; Morgan, M. J.; Kutal, C. *Coord. Chem. Rev.* **2007**, *251*, 515.
- (40) Gardner, A. M.; Wright, T. G. *J. Chem. Phys.* **2011**, *135*, 114305.
- (41) Pickett, T. E.; Richards, C. J. *Tetrahedron Lett.* **1999**, *40*, 5251.
- (42) Roemer, M.; Nijhuis, C. A. *Dalton Trans.* **2014**, *43*, 11815.
- (43) Seiler, P.; Dunitz, J. D. *Acta Crystallogr., Sect. B: Struct. Crystallogr. Cryst. Chem.* **1982**, *38*, 1741.
- (44) Romanov, A. S.; Mulroy, J. M.; Khrustalev, V. N.; Antipin, M. Y.; Timofeeva, T. V. *Acta Crystallogr., Sect. C: Cryst. Struct. Commun.* **2009**, *65*, m426.
- (45) Laus, G.; Wurst, K.; Stolz, W.; Schottenberger, H. *Z. Kristallogr. - New Cryst. Struct.* **2005**, *220*, 239.
- (46) Hnetinka, C. A.; Hunter, A. D.; Zeller, M.; Lesley, M. J. G. *Acta Crystallogr., Sect. E: Struct. Rep. Online* **2004**, *60*, m1806.
- (47) Weigend, F.; Ahlrichs, R. *Phys. Chem. Chem. Phys.* **2005**, *7*, 3297.
- (48) Grimme, S. *J. Comput. Chem.* **2006**, *27*, 1787.
- (49) Oshima, M.; Muraio, T.; Sakurai, Y. *Acad. Rep. Fac. Eng. Tokyo, Poytech. Univ.* **2007**, *30*, 56–59.
- (50) Eckert, F.; Leito, I.; Kaljurand, I.; Kutt, A.; Klamt, A.; Diederhofen, M. *J. Comput. Chem.* **2009**, *30*, 799.
- (51) (a) Boev, V. I.; Dombrovskii, A. V. *Izv. Vyssh. Uchebn. Zaved., Khim. Khim. T.* **1977**, *20*, 1789. (b) Han, Y.-H.; Heeg, M. J.; Winter, C. H. *Organometallics* **1994**, *13*, 3009.
- (52) Khobragade, D. A.; Mahamulkar, S. G.; Pospíšil, L.; Čísařová, I.; Rulíšek, L.; Jahn, U. *Chem. - Eur. J.* **2012**, *18*, 12267.